Available online at www.sciencedirect.com

ScienceDirect

Genomics 89 (2007) 81–88

GENOMICS

www.elsevier.com/locate/ygeno

New insights into gene positional clustering and its properties supported by large-scale analysis of various differentiation pathways

Irena Koutná [a,*], Petr Krontorád [a], Zbyněk Svoboda [a], Eva Bártová [b], Michal Kozubek [a], Stanislav Kozubek [b]

[a] *Center for Biomedical Image Analysis, Faculty of Informatics, Masaryk University, Botanická 68a, 602 00 Brno, Czech Republic*
[b] *Institute of Biophysics, Academy of Sciences, Královopolská 135, 612 65 Brno, Czech Republic*

Received 26 May 2006; accepted 25 July 2006
Available online 25 September 2006

Abstract

To understand how genes are distributed on chromosomes we bring new insights into gene positional clustering and its properties. We have made a large-scale analysis of three types of differentiation and we observed that genes that subsequently enter into different cell processes are positionally clustered on chromosomes. Genes from the clusters are transcribed subsequently with respect to time kinetics and also to position. This means that the genes related to a cellular process are clustered together, independent of the period of time during which they are active and important for the process. Our results also demonstrate not only that there are general regions of increased or decreased levels of gene expression, but also that, in fact, in some chromosome regions we can find clustering of genes related to specific cell processes. The results provided in this paper also support the theory of "transcription factories" and show that transcription of genes from the clusters is managed by softer epigenetic mechanisms.

Keywords: Gene clustering; Differentiation; Microarrays; HL-60; K-562

Gene transcription should not be energetically exhaustive for the cell. The first logical follow-up is that genes required by cellular processes would be clustered on the chromosomes. The second follow-up is that the clusters of genes needed for certain process would be colocalized in the neighborhood of transcription factories [1,2].

Differentiation of cell lines is an excellent experimental model for investigating molecular mechanisms that regulate cellular processes. In the postgenomic era there are many articles covering the area of various types of differentiation. The articles have mostly brought only a list of regulated genes related to certain processes. Our results provide a view on the spatial distribution of genes active during three types of differentiation.

The mapping of active genes to chromosomes showed that genes related to differentiation are mostly localized in regions with increased gene expression (RIDGEs) [3,4], where they form clusters. In these regions there are genes with different time-dependent kinetics. Regulation of these genes is supposed to be driven by epigenetic mechanisms, such as methylation and acetylation [5–13].

Our results suggest a possibility that there are clusters of genes on chromosomes that are controlled by epigenetic mechanisms. To check this, we detected time kinetics of gene expression during several cellular processes. Shapes of the time dependencies reflect the gene regulation mechanisms. The shapes represent the type of regulation, e.g., fast down-regulation. Genes clustered together might be regulated differently for various cellular processes; however, they should remain in clusters. In our experiments, the above-mentioned cellular processes were represented by various types of human cell differentiation.

We compared gene expression profiles obtained during differentiation of HL-60 cells along either the monocyte or the granulocyte pathway and K-562 cells along the megakaryocyte

* Corresponding author. Fax: +420 549 498 360.
E-mail address: qkoutna@fi.muni.cz (I. Koutná).

0888-7543/$ - see front matter © 2006 Elsevier Inc. All rights reserved.
doi:10.1016/j.ygeno.2006.07.013

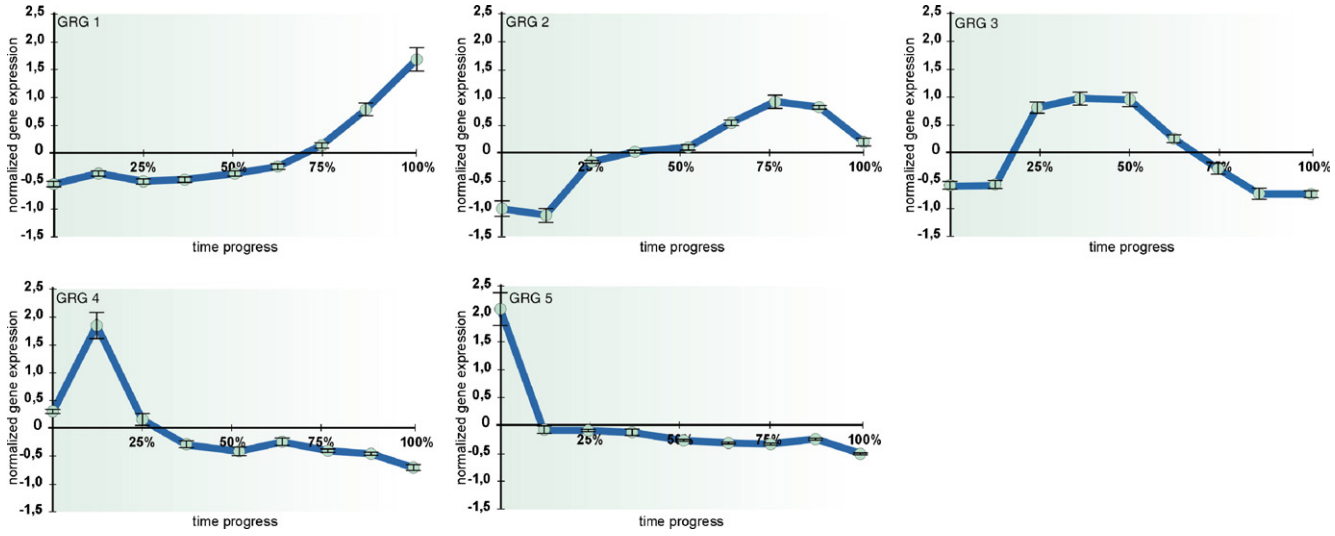

Fig. 1. Self-organizing map (SOM) clustering was used to find five groups of regulated genes (GRG) with distinct time-dependent changes during differentiation. The average values and standard deviations are shown for each data point. The *x* axes represent the sample number, which is proportional to total differentiation time, and the *y* axes represent normalized expression levels (for all differentiation types). Each vector of normalized expression values was normalized (zero mean and standard deviation equal to 1).

differentiation pathway. We used cDNA microarray technology that allowed us to detect consequent changes in gene expression for about 19,000 genes or EST sequences. All regulated genes were divided into five groups of regulated genes (GRG) on the basis of their time-response shape. We realized that there are significant sets of genes belonging to same GRG (i.e., they have the same kinetics) for different differentiations. But we also revealed significant sets of genes belonging to one GRG for one differentiation and to another GRG for another differentiation. In other words, genes in these subsets behaved similarly during one differentiation.

Results

We analyzed time-dependent changes in gene expression profiles during monocytic (MD) and granulocytic (GD) differentiation of HL-60 cells or megakaryocytic (MKD) differentiation of K562 cells using cDNA microarrays. The stage of differentiation was determined according to the expression of CD11b in GD, CD14 and CD11b in the case of MD, and CD44 during MKD, using flow-cytometric analysis. We identified 4718 (MD), 4505 (GD), and 4947 (MKD) genes with differential expression for the chosen discrimination level.

We performed cluster analysis and we obtained five GRG containing genes from each type of differentiation (characteristic expression profiles for each GRG are shown in Fig. 1). It is interesting to note that there were practically no initially down-regulated genes that would be up-regulated in terminally differentiated cells. The numbers of genes or ESTs in GRG

Table 1
Groups of regulated genes (GRG) in various differentiation processes

Type of differentiation	Number of genes inside each GRG for relevant differentiation				
	1	2	3	4	5
Monocyte (MD)	967	492	1038	680	683
Granulocyte (GD)	856	856	528	887	856
Megakaryocyte (MKD)	615	859	874	677	684

The numbers of genes inside the five GRG for GD, MD, and MKD are shown.

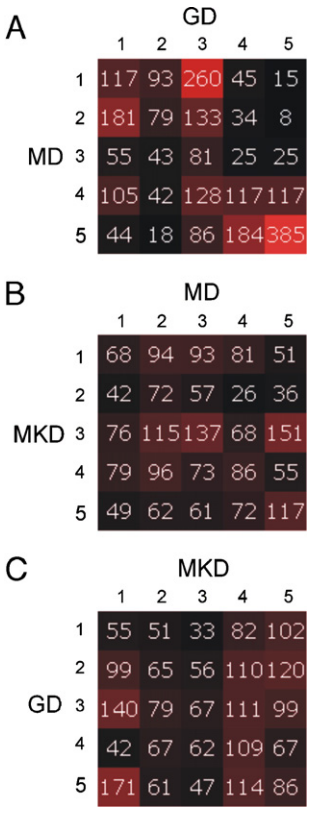

Fig. 2. Intersections of groups of regulated genes between individual differentiation processes. (A) MD and MKD, (B) GD and MD, and (C) GD and MKD. For better visualization of individual intersections we colored each box using a relevant amount of red (the more intense the color, the more genes in the intersection).

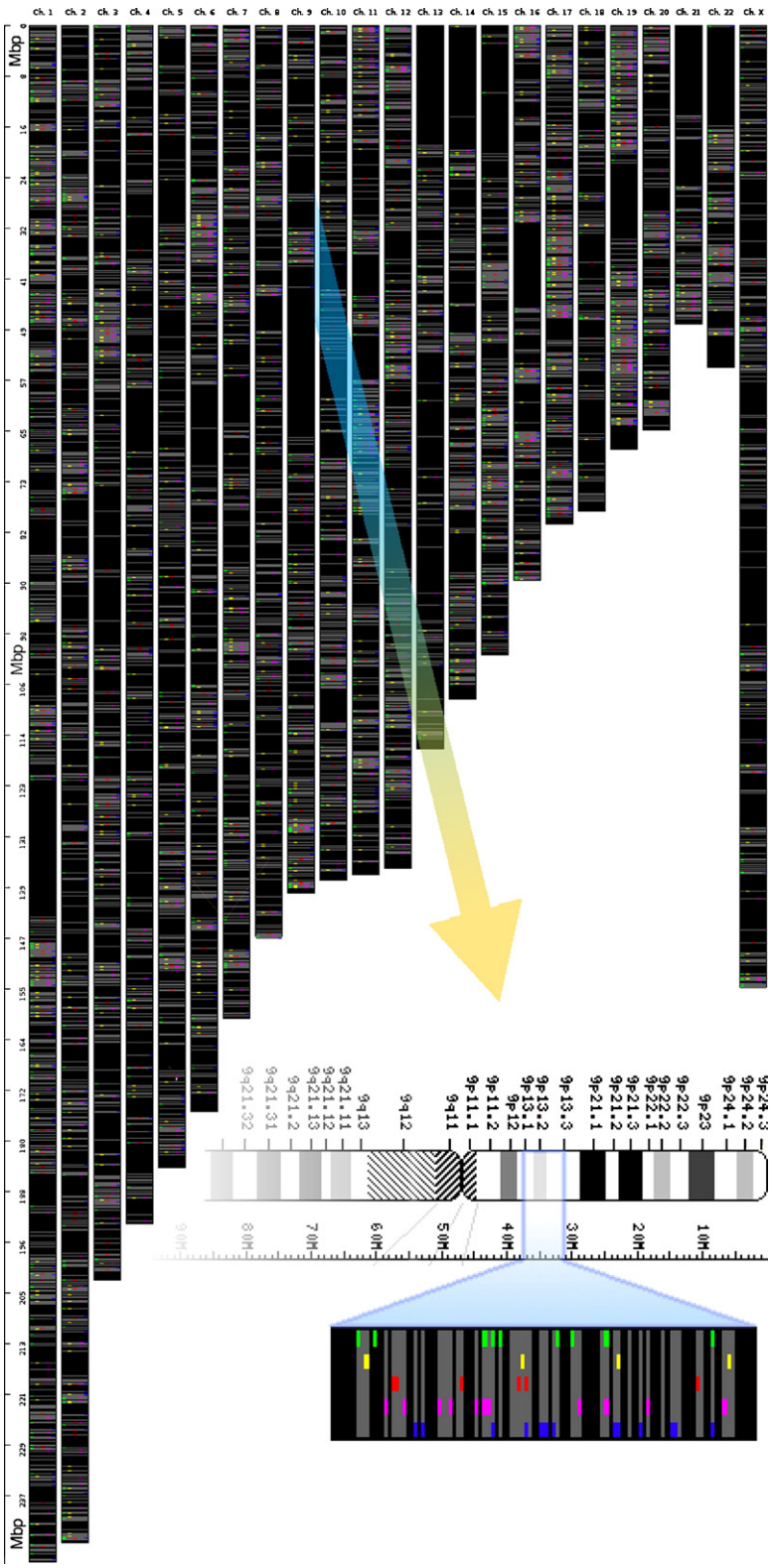

Fig. 3. Granulocytic differentiation of HL-60 cells is taken as an illustrative example showing the distribution of genes or ESTs of various GRG on human chromosomes. The different color ticks represent genes or ESTs of the five GRG (1, green; 2, yellow; 3, red; 4, magenta; 5, blue). Gray ticks represent all spotted sequences of our cDNA microarrays (about 19,000 genes or ESTs). The thickness of the ticks is 0.1 Mb for the detailed area of chromosome 9 and 0.5 Mb for the rest of the image. Therefore, in some cases, ticks of different color may appear at the same vertical distance—this is caused by mapping resolution.

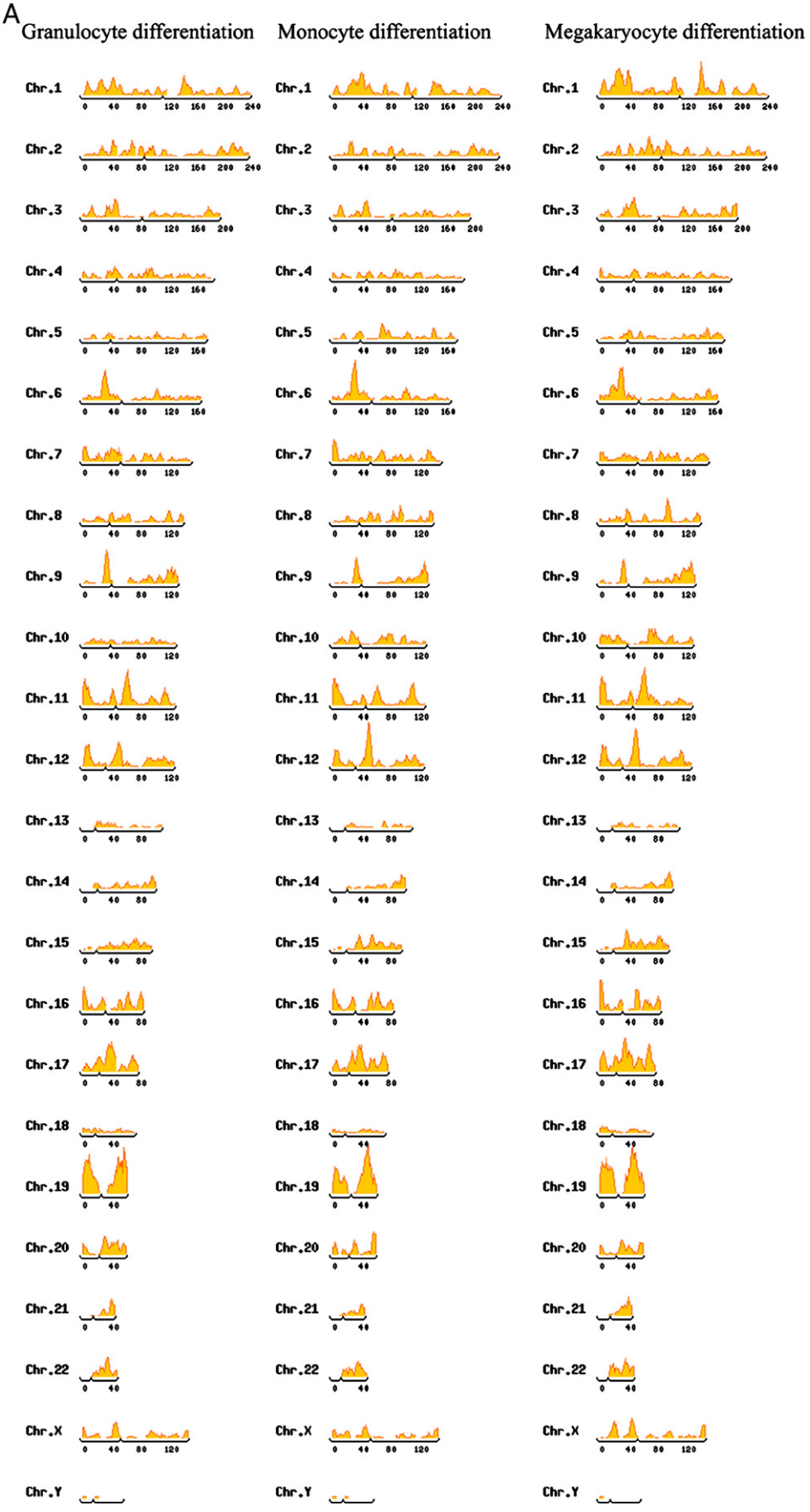
A
Granulocyte differentiation
Monocyte differentiation
Megakaryocyte differentiation
Chr.1
Chr.2
Chr.3
Chr.4
Chr.5
Chr.6
Chr.7
Chr.8
Chr.9
Chr.10
Chr.11
Chr.12
Chr.13
Chr.14
Chr.15
Chr.16
Chr.17
Chr.18
Chr.19
Chr.20
Chr.21
Chr.22
Chr.X
Chr.Y

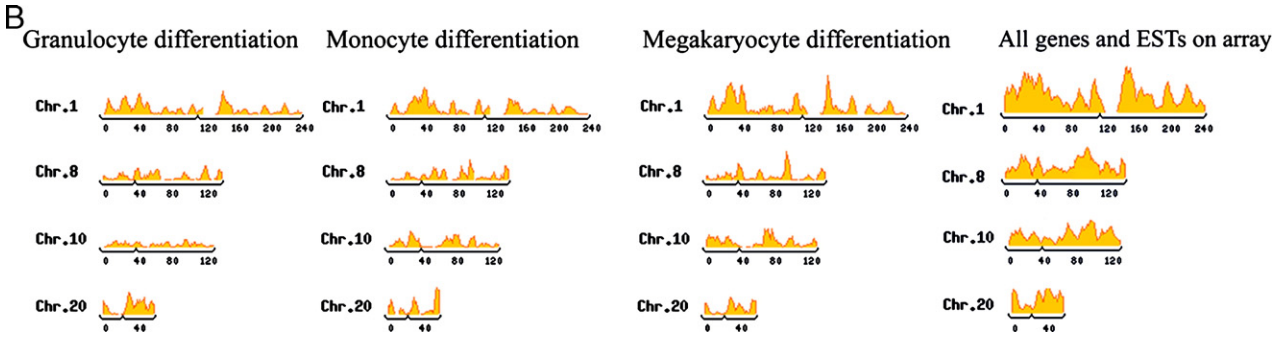

Fig. 4. Density of regulated genes ($R \times R/T$, see Materials and methods) for different types of differentiation processes. (A) One can clearly see the regions with high density of regulated genes and also with large absolute numbers of regulated genes. (B) The density of regulated genes in general does not reflect the initial gene density obtained from the microarray slide used. For each plot, the horizontal axis represents position in Mb and the vertical axis represents the density.

for all types of differentiation are shown in Table 1. Each characteristic profile represents one type of regulation kinetic, e.g., GRG 1 represents genes with nondecreasing expression.

In our further analysis we projected the GRG of different pathways into each other. The numbers of genes found simultaneously in the *n*th GRG of MD and at the same time in the *m*th GRG of GD are shown in Fig. 2A. Similarly, mutual projections of MD vs MKD and MKD vs GD are shown in Figs. 2B and 2C. For example, 385 genes (56%) of the GD GRG 5 (slow up-regulation) are shared with GRG 5 of MD. In some cases, the same genes can be found in GRG with different kinetics for different differentiations. For example, 171 genes (28%) are common to GRG 1 from GD and GRG 5 from MKD.

When we focused on regions with a high density of regulated genes, we saw the occurrence of genes from all five GRG along the chromosomes (Fig. 3). We found many nice examples of positional repetition of regulated genes along chromosomes.

Further evaluation of the data provided by the visualization of weighted area regulation (see Materials and methods) confirmed that regulated genes are nonrandomly scattered on chromosomes. In addition, the distribution of regulated genes varies among the investigated types of differentiation (Figs. 4A and 4B). For example, positional clustering of genes regulated in GD and MD can be seen at the first 10 Mb of chromosome 7. In contrast, there is no cluster in this region for MKD. On chromosome 8, around 90 Mb, we can find 35% of genes regulated in MKD instead of 10% in GD. Many similar examples can be found in Fig. 4A. The density of regulated genes in general does not reflect the initial gene density obtained from the whole microarray (Fig. 4B). For example, only 5 of about 60 genes are regulated in the MD at the area around 30 Mb on chromosome 20. The occurrence of regulated genes in various RIDGEs is not uniform and distinct differentiation processes involve genes that occupy different parts of RIDGEs. These results provide further nice evidence of gene clustering along chromosomes entering various types of differentiation.

To confirm the reliability of microarray data, RT-PCR was performed using eight genes with altered expression (four down-regulated and four up-regulated). The RT-PCR confirmed the same patterns of gene expression as cDNA microarrays for all tested genes. Although the level of gene expression determined by cDNA microarrays was not identical to the level of gene expression obtained with RT-PCR, both methods indicated similar patterns of gene expression changes (Fig. 5 and Table 2).

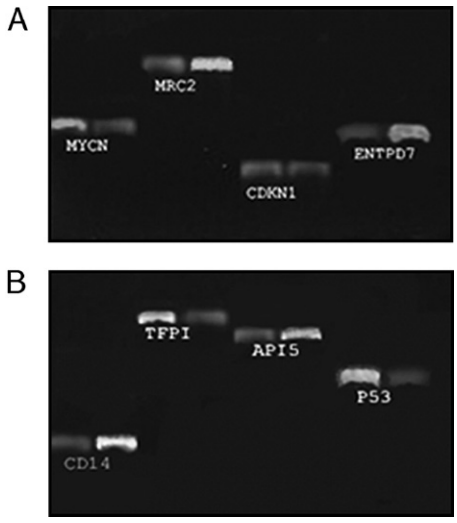

Fig. 5. RT-PCR analysis of 2% agarose gel performed to check regulation patterns obtained using microarray technique. (A) Granulocyte differentiation and (B) monocyte differentiation are shown.

Discussion

We revealed positional clustering of genes related to three types of ex vivo differentiation—differentiation of HL-60 into granulocytes and monocytes and K-562 into megakaryocytes. Caron et al. proved the existence of RIDGE domains on chromosomes. We found subgroups of genes inside RIDGE domains that are closely connected with special cell processes. This is a very important demonstration that, from the functional point of view, there are not only regions of increased or decreased levels of gene expression but also groups of genes related to some cellular processes. Our visualizations show the positional clustering of regulated genes on chromosomes. Regulated genes (see in Materials and methods) were divided into five GRG according to the time

Table 2
Expression profiles of selected genes during two differentiation processes

Gene	GRG No. for relevant differentiation	Gene expression levels at relevant time points of differentiation (h)								
GD		0	18	36	54	72	90	108	126	144
MYCN	5	6031	269	244	-	187	180	176	207	206
MRC2	1	1486	1594	1564	1539	1334	1525	1397	4316	15,230
CDKN1A	5	3201	2658	2555	2432	3031	1121	1026	1081	996
ENTPD7	1	1206	1428	1331	1243	1240	1238	7234	11,201	25,870
MD		0	9	18	27	36	45	54	63	72
CD14	1	1583	1629	1935	2381	4024	5228	15,621	20,528	35,062
TFPI	5	19,039	1664	1402	1379	1355	1385	1415	1445	1437
API5	1	1619	1670	2194	6349	10,503	8442	6349	14,321	16,571
P53	5	20,767	1719	16,571	1479	13,027	1662	1296	1931	1593

Every number represents the normalized level of expression at the relevant time point of differentiation.

kinetics of gene expression changes. These groups were sorted according to the occurrence of maximum expression (Fig. 1). The number of genes in particular GRG fluctuated between 500 and 1000 (Table 1). When we projected the genes from GRG onto chromosomes we obtained territories (inside RIDGEs) accumulating genes of various functions and time kinetics but connected with distinct differentiation processes (Fig. 3). We will refer to these territories as positional clusters. We realized that there are no positional clusters containing genes from only a single GRG. One can see a system in the distribution of GRG genes inside positional clusters. This system reflects the dynamics of gene regulation changes without energy-consuming chromatin reorganization. Consequently switches to needed genes are probably managed by mechanisms on the epigenetic regulation level. Clustering of genes also supports energetically profitable switching of genes being transcribed in "transcription factories"—there is no need for wide transfers.

To compare various groups of genes with similar (or different) regulation in the differentiation pathways (mentioned above), we calculated the intersections of GRG. These calculations resulted in two-dimensional tables (Fig. 2). Using these tables we revealed that there are GRG in principle shared by differentiation types (e.g., 385 genes for GD/MD shared by GRG 5). We also revealed that there are groups of genes in common for two differentiation types but with different time kinetics. This means that there are groups of active genes used differently during different differentiations (e.g., 171 genes shared by GRG 1 for MKD and GRG 5 for GD). In other words, regulated genes form groups; genes in these groups behave similarly during one differentiation process. But the behavior of genes in the clusters can vary between different differentiation processes. For example, GRG that are up-regulated during one differentiation can be down-regulated during another differentiation.

In comparison with other authors this study works with about 19,000 genes/ESTs during three types of differentiation. Our study follows and confirms studies involving from 872 to 12,500 genes/ESTs [28–31] mostly during one type of cellular process. An interesting fact is that our results correlate with conclusions presented by studies performed on another species [32].

The results presented in our study are important for better understanding of changes in gene expression. The differentiation pathways appeared to be an appropriate way to study differences in transcription of genes. Furthermore, characterizations of regions entering various cell processes using powerful microarray technology, as shown in this paper, bring new views of the genome related to transcriptional regulation.

Materials and methods

Cell cultivation and differentiation

The human promyelocytic leukemia HL-60 and human erythroleukemia K562 cell lines were grown in logarithmic phase in RPMI medium supplement with 10% heat-inactivated fetal bovine serum, 100 U/ml penicillin, 100 μg/ml streptomycin, and 20 mM glutamine at 37°C in a humidified atmosphere and 5% CO_2.

Cell differentiation

Monocytic differentiation of HL-60 cells was induced by phorbol 12-myristate 13-acetate (PMA; 100 μM) (Sigma) for 72 h. HL-60 cells were

Table 3
Overview of primers used for control PCR experiments

Gene	Primer	Primer sequence
ENTPD7	Forward	5′-AATCTACCTTTTCTTCCCTTGC-3′
	Reverse	5′-ACTACGACAGGGATCTTGGATCA-3′
MRC2	Forward	5′-ATGGGATCTGCCAGTTGC-3′
	Reverse	5′-CAGGACTGAGACGTTGAGACC-3′
CDKN1A	Forward	5′-GCCGGAGCTGGGCGCGGATT-3′
	Reverse	5′-CTGAGACTAAGGCAGAAGAT-3′
MYCN	Forward	5′-GGCAGTAGGACCACCAGTGT-3′
	Reverse	5′-CTAATACTGGCCGCAAAAGC-3′
CD14	Forward	5′-AGGACTTGCACTTTCCAGCTTG-3′
	Reverse	5′-TCCCGTCCAGTGTCAGGTTATC-3′
TFPI	Forward	5′-GATCCTGGAATATGTCGAGGT-3′
	Reverse	5′-TCTTGCATTCTTCCAGTGTCT-3′
API5	Forward	5′-TTTAGGTGGGTTGTTCAGCC-3′
	Reverse	5′-TTCTAGGACCTTTTTGGATTCA-3′
P53	Forward	5′-GAGGTTGTGAGGCGCTGCCCC-3′
	Reverse	5′-TTCCTCTGTGCGCCGGTCTCT-3′

incubated with DMSO (1.25% (v/v)) for 6 days to induce granulocytic differentiation. Megakaryocytic differentiation of K562 cells was carried out using 100 μM PMA for 72 h [14,15].

DNA microarrays

Microarray slides used in this study (SS-H19k6 QuantArray; Clinical Genomic Centre, Toronto, ON, Canada) contained 19,200 human cDNAs, positive controls (fragments of the *Arabidopsis* chlorophyll synthetase gene that has no homology to any human gene), and negative controls (3× SSC). Experiments were repeated twice for each time point and each type of differentiation with similar results. In the final analysis, the mean values of intensity from different measurements were taken for each spot. Spots were excluded from later measurements if their difference in normalized intensities was higher than 25%.

Probe preparation, hybridization, and washing

For each microarray experiment 10 to 20-μg samples of purified total RNA were labeled by incorporating Cy3- and Cy5-dCTP (Amersham) using oligo(dT) primers (anchored) and SuperScript II (Invitrogen) during RT-PCR. The acquired labeled cDNA was precipitated by isopropanol (protocols from the OCI Microarray Centre, 2000). Before hybridization, each slide was incubated in blocking solution (5× SSC, 0.1% SDS, and 10 mg/ml BSA) at 37°C for 1 h. Slides were incubated in 30 μl of hybridization solution (DIG Easy Hyb Granules; Roche) containing Cy3- and Cy5-labeled target, 5 μl of yeast tRNA (Invitrogen), and 5 μl of calf thymus DNA (Life Technologies). Hybridization was performed by the incubation of slides in the hybridization chamber overnight at 37°C. Next day, the slides were washed three times in 1× SSC with 0.1% SDS for 10 min at 50°C. After washing, the samples were rinsed in 1× SSC (according to protocols from the OCI Microarray Centre, 2000).

Semiquantitative RT-PCR

Total RNA samples were reverse transcribed to single-stranded cDNA using oligo(dT) primers (anchored) with SuperScript II reverse transcriptase (Invitrogen). Each diluted cDNA was used as a template for subsequent PCR amplification. Each PCR was carried out in a 50-μl volume of master mix with 1 mM $MgCl_2$ and *Taq* DNA polymerase, for 5 min at 94°C for initial denaturing, followed by 10, 15, 20, 25, 30, and 35 cycles of 30 s at 94°C, 30 s at 52 to 60°C according to the used primer, and 1.5 min at 72°C, in the PCR system (PTC-100; MJ Research, Inc.). Results of RT-PCR were confirmed by agarose gel electrophoresis and evaluated by Gene Tools v3.00.22 (SynGene). 18Sr RNA served as an internal control for comparison of equal amounts of expression of tested genes [16].

Using RT-PCR we confirmed the changed expression of eight genes detected by microarrays. RT-PCR was performed on the group of four genes from monocyte differentiation and four genes from granulocyte differentiation. Every group contained two up and two down regulated genes correspondent with time 0 (non affected cells) versus end point of relevant type of differentiation. For RT-PCR we have chosen the genes with significant change of expression. We have chosen MYCN, CDKN1A to check down-regulation and MRC2 and ENTPD7 to check up-regulation during granulocyte differentiation (Fig. 5A). Genes CD14 and API5 were used to check up-regulation, genes P53 and TFPI were used to check down-regulation during monocyte differentiation (Fig. 5B). See Table 3 for a list of the primers used.

Image analysis and data processing

To analyze images produced by the microarray scanner, we used software developed in our laboratory within our research performed in the microarray data processing area. The grid was semiautomatically set up for each image and the alignment to the array of spots was carefully checked. Each spot was segmented individually in its surroundings by the gradient weighted segmentation method [17] and the quality analysis was automatically performed. This procedure removed some defective spots according to their shapes (circularity) and intensity distributions in the foreground area. Our image analysis method is very similar to those used by commercial software packages. The spots were quantified by taking the mean of the intensities of the foreground pixels. The local background intensity for each spot was determined as the mean of the background area. The background was subtracted from the foreground intensity.

The next stage of data analysis was the normalization of the measured intensity values. Our aim was to evaluate gene expression at particular time points in time-series experiment so we chose the single-channel analysis technique. This normalization allows comparisons of absolute intensities between arrays. Single-channel normalization of two-color cDNA microarray experiments can be considered as a two-stage process: within-slide normalization followed by between-slide normalization. We applied print-tip LOWESS [18] for within-slide normalization. This method allowed us to suppress spatial- and intensity-dependent bias. The smoothing parameter was set to 0.33. Then the between-slide normalization was performed using quantile normalization proposed by Bolstad [19]. Both mentioned methods were implemented within our research performed in the microarray data processing area.

We performed cluster analysis of results to obtain groups of similarly expressed genes.

There is a large number of existing clustering methods but unfortunately there are no decisive criteria for selecting the most optimal one [20]. Different approaches [21] were tried, *K*-means, SOM [22], and *C*-means, and results were very similar. We chose the SOM due mainly to its advantages mentioned, e.g., in [23]. GeneCluster2 [24] was chosen for the computations and visualization of the results. In the first step, called data preprocessing, genes or ESTs that were differentially expressed across time were selected using a variation filter. For the selection, a relative change of 1.5-fold and an absolute change of 500 units were set.

Choosing the number of clusters is the most critical step of cluster analysis, even more critical then choosing the clustering method. There exists a theory dealing with this task (see [21,25] for details). The number of clusters can be validated by different classification methods [26]. A robust approach combining different classification methods by "voting" [27] was chosen. The number of clusters (5) was not chosen arbitrarily. Based on the mentioned calculations the most optimum number of clusters for our dataset is 5. Thus, after within-slide normalization, SOM with 500,000 iterations was applied to genes that passed the variation filter to create five groups of genes with similar regulation (the GRG).

Genes from all clusters were mapped on chromosomes according to their position in base pairs and chosen resolution (genes were mapped proportionally to image height). Each cluster was assigned one color and each gene was painted using the color of its cluster. We used gray to highlight all studied genes (all genes printed to our microarrays). To increase expression potency of the visualization, each cluster was assigned a single column in the chromosome (leftmost column represents cluster 1, rightmost column cluster 5). Fig. 3 is an example of such visualization.

The occurrence of regulated genes along chromosomes is influenced by the positional distribution of genes spotted on our arrays. Therefore, for visualization of the spatial distribution of regulated genes, the following technique called weighted area regulation was used. We computed the spatial occupancy of all genes printed on our arrays on chromosomes using a sliding window of given width in base pairs. Evaluation of the number of genes for each sliding window position resulted in vector T for each chromosome (i.e., each item in the vector is the number of genes within the sliding window moved by the appropriate distance). The length of T is proportional to the current chromosome length. We performed the same computation for the regulated genes only, resulting in vector R. Scalar division of these two vectors (R/T) gave us the vector of densities of regulated genes with respect to our arrays. These densities, however, strongly fluctuated for regions with low gene numbers. Therefore, to conserve the advantages of both quantities R and R/T, the multiplication $R \times R/T$ was calculated (R/T was used as a weight vector for visualization of the vector R). The resulting values express the amount of regulated genes in a given region weighted by the density of all regulated genes in the region. We plotted this computation for each chromosome (Fig. 4). One can clearly see the regions with a high density of regulated genes and with a large absolute number of regulated genes. Our method combines both relative and absolute numbers.

Acknowledgments

This work was generously supported by the Grant Agency of the Ministry of Health of the Czech Republic (Grant 1A/8241-3), the Ministry of Education of the Czech Republic (Grant MSM-0021622419, LC535), the Grant Agency of the Czech Republic (Grant 301/04/P136, 2204/0907), and the Grant Agency of the Academy of Science of the Czech Republic (Grant IAA5004306).

References

[1] C.S. Osborne, et al., Active genes dynamically colocalize to shared sites of ongoing transcription, Nat. Genet. 36 (2004) 1065–1071.
[2] L. Chakalova, E. Debrand, J.A. Mitchell, S.C. Osborne, P. Fraser, Replication and transcription: shaping the landscape of the genome, Nat. Rev. Genet. 6 (2005) 669–678.
[3] H. Caron, B. van Schaik, M. van der Mee, F. Baas, G. Riggins, P. van Sluis, M.C. Hermus, R. van Asperen, K. Boon, P.A. Voute, S. Heisterkamp, A. van Kampen, R. Versteeg, The human transcriptome map: clustering of highly expressed genes in chromosomal domains, Science 291 (2001) 1289–1292.
[4] R. Versteeg, B.D.C. Schik, M.F. Batenburg, M. Roos, R. Monajemi, H. Caron, H.J. Bussemaker, A.H.C. van Kampen, The human transcriptome map reveals extremes in gene density, intron length, GC content, and repeat pattern for domains of highly and weakly expressed genes, Genome Res. 13 (2003) 1998–2004.
[5] T. Cremer, C. Cremer, Chromosome territories, nuclear architecture and gene regulation in mammalian cells, Nat. Rev. Genet. 2 (2001) 292–301.
[6] J. Croft, et al., Differences in the localization and morphology of chromosomes in the human nucleus, J. Cell Biol. 145 (1999) 1119–1131.
[7] E. Bartova, et al., Nuclear topography and expression of the BCR/ABL fusion gene and its protein level influenced by cell differentiation and RNA interference, Leuk. Res. (2005) 901–913.
[8] E. Lukášova, S. Kozubek, M. Kozubek, M. Falk, J. Amrichova, The 3D structure of human chromosomes in cell nuclei, Chromosome Res. 10 (2002) 535–548.
[9] I. Volpi, et al., Postgrafting administration of granulocyte colony-stimulating factor impairs functional immune recovery in recipients of human leukocyte antigen haplotype-mismatched hematopoietic transplants, Blood 97 (2001) 2514–2521.
[10] S. Chambeyron, W.A. Bickmore, Chromatin decondensation and nuclear reorganization of the HoxB locus upon induction of transcription, Genes Dev. 10 (2004) 1119–1130.
[11] M. Skalnikova, et al., Spatial arrangement of genes, centromeres and chromosomes in human blood cell nuclei and its changes during the cell cycle, differentiation and after irradiation, Chromosome Res. 8 (2000) 487–499.
[12] I. Koutna, et al., Topography of genetic loci in tissue samples: towards new diagnostic tool using interphase FISH and high-resolution image analysis techniques, Anal. Cell. Pathol. 20 (2000) 173–185.
[13] S. Kozubek, et al., 3D structure of the human genome: order in randomness, Chromosoma 111 (2002) 321–331.
[14] S. Depraetere, M. Joniau, Polar agents with differentiation-inducing capacity prime myelomonocytic cell lines to lipopolysaccharide-induced cytolysis: the role of endogenous tumor necrosis factor, Leukemia 8 (1994) 1951–1959.
[15] S. Depraetere, B. Vanhaesebroeck, W. Fiers, J. Willems, M. Joniau, Polar agents with differentiation inducing capacity potentiate tumor necrosis factor-mediated cytotoxicity in human myeloid cell lines, J. Leukocyte Biol. 57 (1995) 141–151.
[16] S. Selvey, E.W. Thompson, K. Matthaei, R.A. Lea, M.G. Irving, L.R. Griffiths, Beta actin, an unsuitable internal control for RT-PCR, Mol. Cell. Probes 15 (2001) 307–311.
[17] C. MacAulay, B. Palcic, A comparison of some quick and simple threshold selection methods for stained cells, Anal. Quant. Cytol. Histol. 10 (1988) 134–138.
[18] Y.H. Yang, N. Thorne, Normalization for two-color cDNA microarray data, in: D. Goldstein (Ed.), A Festschrift for Terry Speed, IMS Lecture Notes, Monogr. Ser., 40, 2003, pp. 403–418.
[19] B.M. Bolstad, R.A. Irizarry, M. Åstrand, T.P. Speed, A comparison of normalization methods for high density oligonucleotide array data based on variance and bias, Bioinformatics 19 (2003) 185–193.
[20] G.J. McLachlan, K. Do, C. Ambroise, Analyzing Microarray Gene Expression Data, Wiley–Interscience, New York, 2004.
[21] F. Azuaje, N. Bolshakova, Clustering genome expression data: design and evaluation principles, in: D. Berrar, W. Dubitzky, M. Granzow (Eds.), Understanding and Using Microarray Analysis Techniques: A Practical Guide, Springer-Verlag, London, 2002.
[22] T. Kohonen, The self-organizing map, Proc. IEEE 78 (1990) 1464–1480.
[23] P. Tamayo, Interpreting patterns of gene expression with self-organizing maps: methods and application to hematopoietic differentiation, Proc. Natl. Acad. Sci. USA 16 (1999) 2907–2912.
[24] M. Reich, K. Ohm, P. Tamayo, M. Angelo, J.P. Mesirov, GeneCluster 2.0: An advanced toolset for bioarray analysis, Bioinformatics (2004) doi:10.1093/bioinformatics/bth138.
[25] N. Bolshakova, F. Azuaje, P. Cunningham, An integrated tool for microarray data clustering and cluster validity assessment, Bioinformatics 21 (2005) 451–455.
[26] J.C. Bezdek, N.R. Pal, Some new indexes of cluster validity, IEEE Trans. Syst. Man Cybernet. 28 (1998) 301–315.
[27] N. Bolshakova, F. Azuaje, Estimating the number of clusters in DNA microarray data, Methods Inf. Med. 45 (2006) 153–157.
[28] H.F. Juan, Biomic study of human myeloid leukemia cells differentiation to macrophages using DNA array, proteomic, and bioinformatic analytical methods, Electrophoresis 15 (2002) 2490–2504.
[29] S.L. Pomeroy, P. Tamayo, et al., Prediction of central nervous system embryonal tumour outcome based on gene expression, Nature 415 (2002) 436–442.
[30] J. Seo, M. Kim, J. Kim, Identification of novel genes differentially expressed in PMA-induced HL-60 cells using cDNA microarrays, Mol. Cells 10 (2000) 733–739.
[31] K.H. Lee, et al., Differential gene expression in retinoic acid-induced differentiation of acute promyelocytic leukemia cells, NB4 and HL-60 cells, Biochem. Biophys. Res. Commun. 296 (2002) 1125–1133.
[32] Q. Li, B. Lee, L. Zhang, Genome-scale analysis of positional clustering of mouse testis-specific genes, BMC Genom. 6 (2005) 1–7.